Supporting information

Boosting Cancer Immunotherapy by an Biomineralized Nanovaccine with Ferroptosis-Inducing and Photothermal Properties

Siyu Ma, Xiao Liang, Ning Yang, Jie Yang, Jun Zhang, Xiuhua Pan, Yawen Wei, Zengyi Liu, Qi Shen *

Affiliations：

School of Pharmacy, Shanghai Jiao Tong University, 800 Dongchuan Road, Shanghai 200240, China

Corresponding author details:

Qi Shen

School of Pharmacy, Shanghai Jiao Tong University, 800 Dongchuan Road, Shanghai 200240, China

Tel: +86-21-34204049

Fax: +86-21-34204049

E-mail: qshen@sjtu.edu.cn

Supplementary Data and Figures

	Encapsulation Effciency for $Fe(OH)_3$	Drug-Loading Rate for $Fe(OH)_3$	Encapsulation Effciency for IR820	Drug-Loading Rate for IR820
Fe@OVA-IR820	41.99±2.37%	11.97±0.67%	50.04±3.48%	1.87±0.13%

Figure S1. Encapsulation rate and drug loading rate of Fe@OVA-IR820 nanovaccine to $Fe(OH)_3$ and IR820.

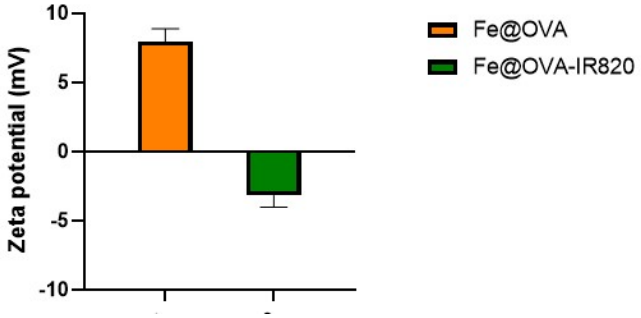

Figure S2. Zeta potential of Fe@OVA and Fe@OVA-IR820.

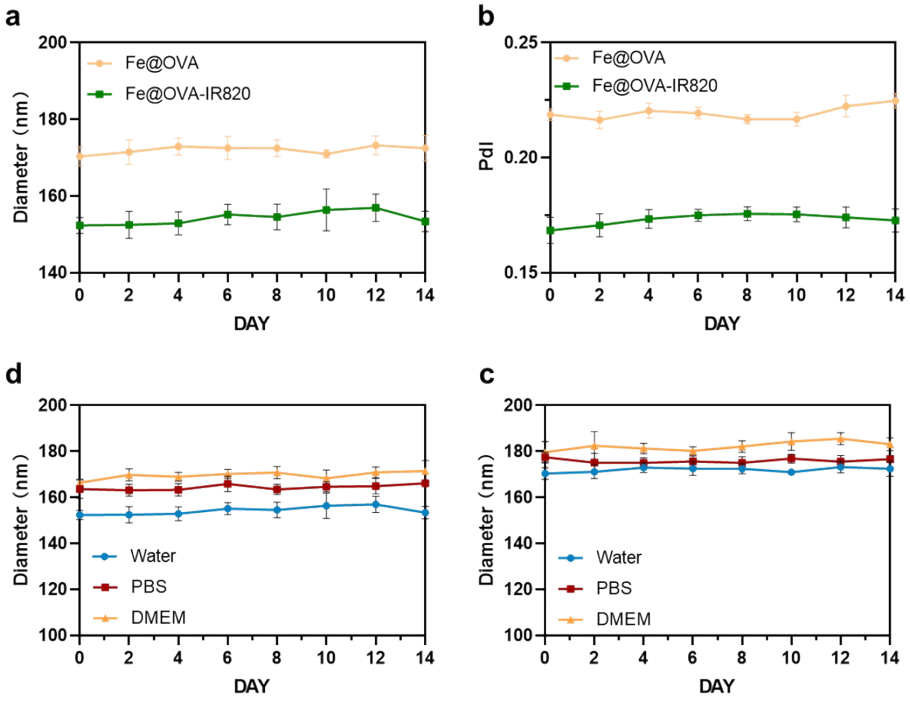

Figure S3. The stability of prepared nanoparticles at 4 °C for 14 days. The particle size (a) and PDI (b) were determined. The stability of the stability of Fe@OVA - IR820 (c) and Fe@OVA (d) in various physiological solutions was recorded.

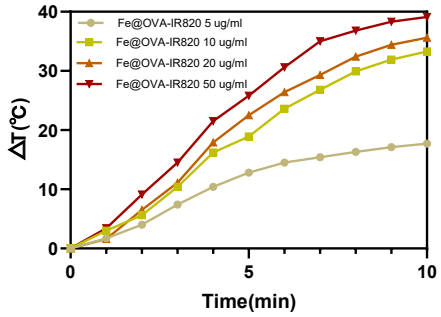

Figure S4. The rising temperature with different concentrations of Fe@OVA-IR820 under laser irradiation.

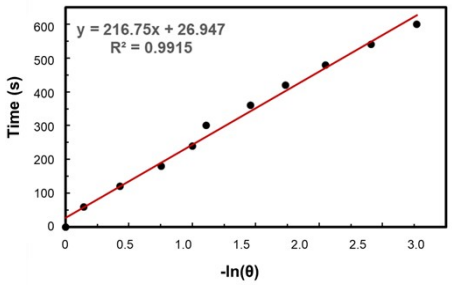

Figure S5. Plot and linear fit of time versus negative natural logarithm of the temperature increment for the cooling rate of Fe@OVA-IR820 solution.

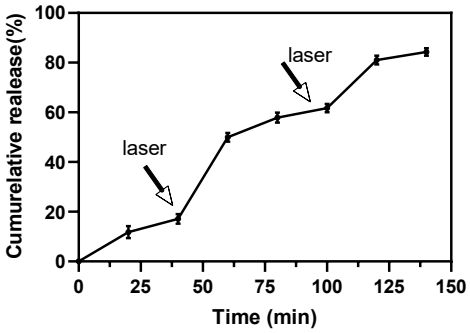

Figure S6. In vitro cumulative iron ions from nanovaccines incubated with PBS (pH 5.0) at 37°C upon 5 min 808 nm laser irradiation (n = 3).

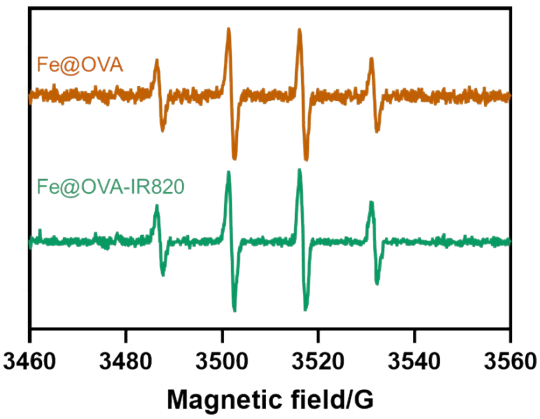

Figure S7. ESR spectra of nanopartical-generated •OH (experimental conditions: DMPO concentration of 100 mM, and trapping time of 10 min).

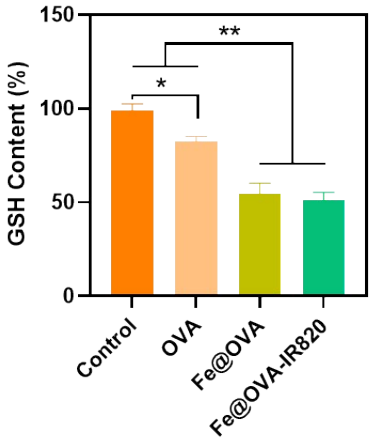

Figure S8. Content of GSH after treatment with different preparations.

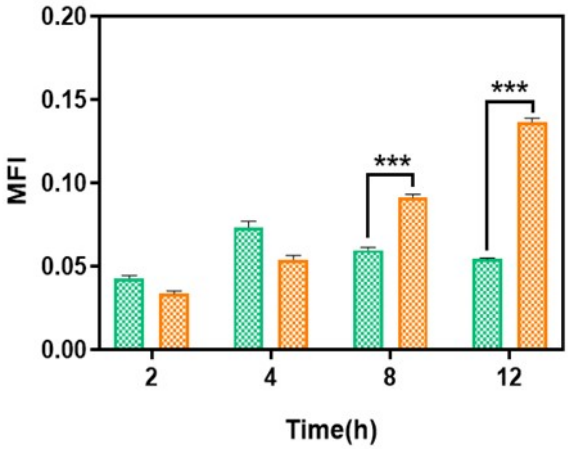

Figure S9. Fluorescence semi-quantitative analysis of IR820 signal in Fig.2A (n = 3).

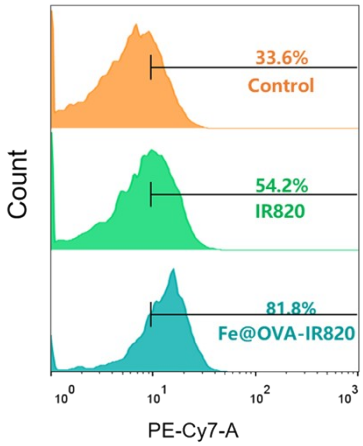

Figure S10. Cellular uptake of free IR820 and Fe@OVA-IR820 in NIH-3T3 cells detected by flow cytometry after 12 hours of incubation.

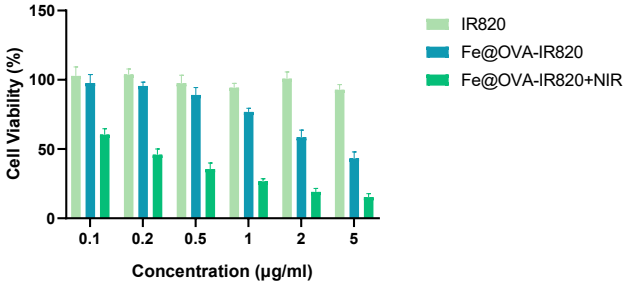

Figure S11. Relative viabilities of NIH-3T3 cells after incubated 12h and irradiated for 5 minutes.

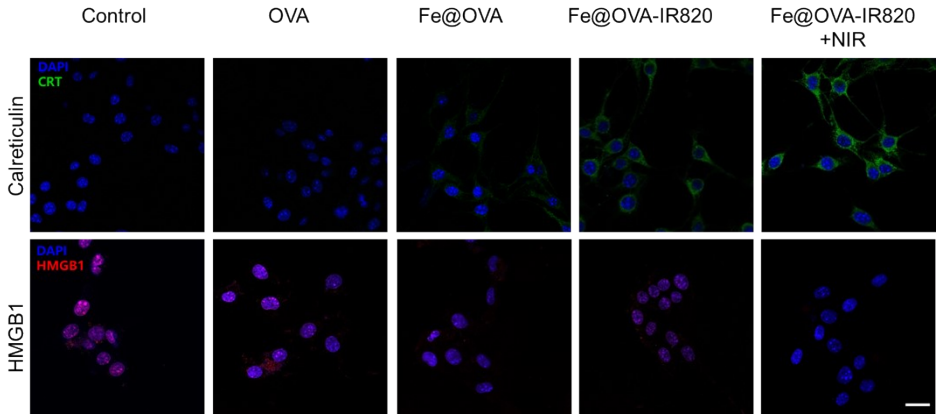

Figure S12. Immunofluorescence signal acquisition of calreticulin (above) and HMGB1 (below). Scale, 50 μm.

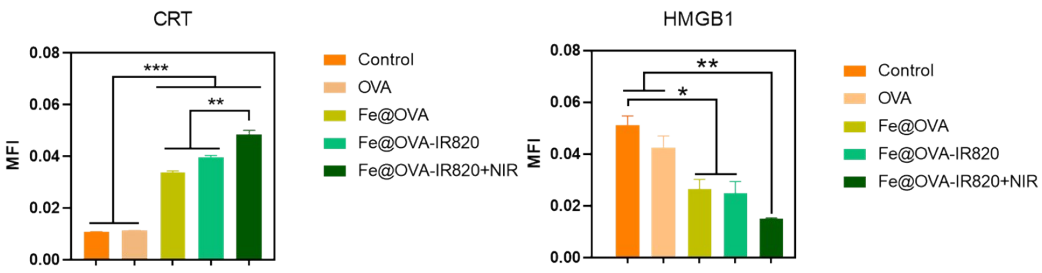

Figure S13. The fluorescence semi-quantification of CRT (upside) and HMGB1 (below) signal in respectively.

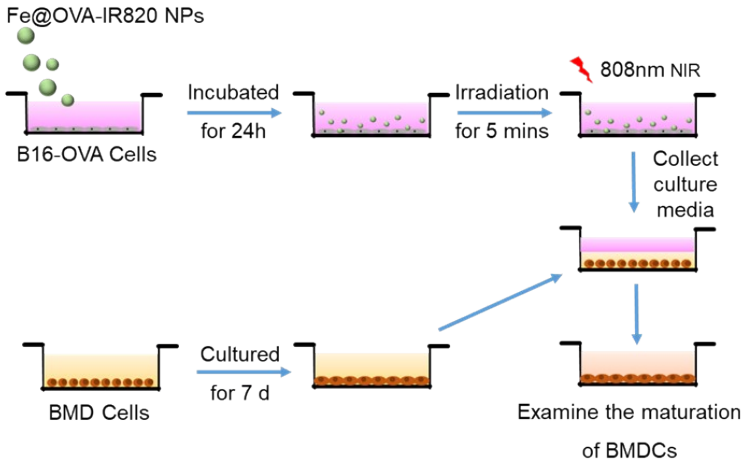

Figure S14. Schematic illustration of stimulating the maturation of bone marrow-derived cells (BMDCs). CD11c-positive dendritic cells were gated by flow cytometry.

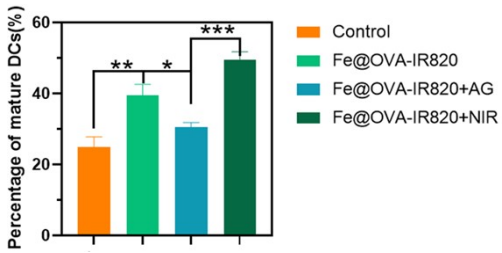

Figure S15. Percentage of mature DC cells of Figure 3G.

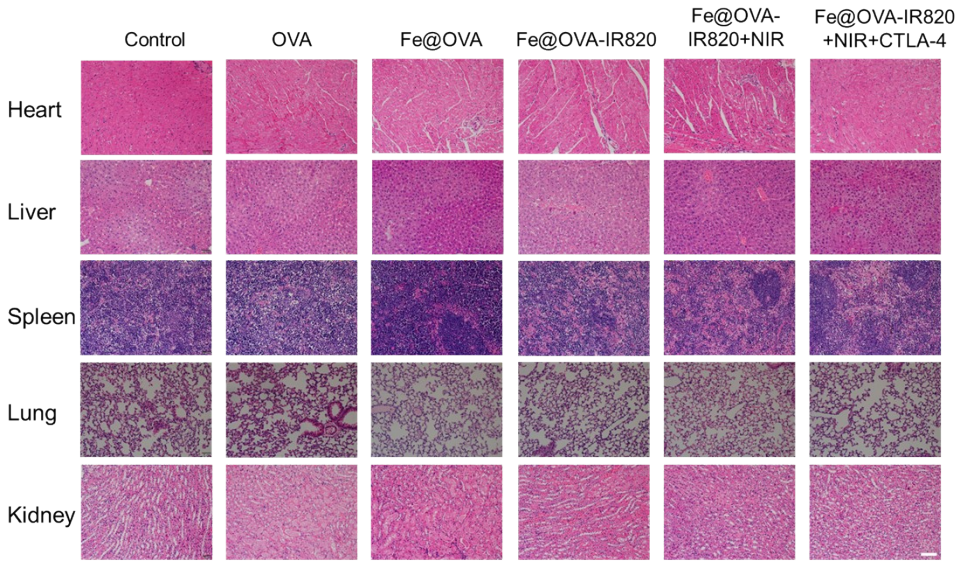

Figure S16. H&E staining of major organs at the end of anti-tumor efficacy experiment, scale bars are 100 μm.

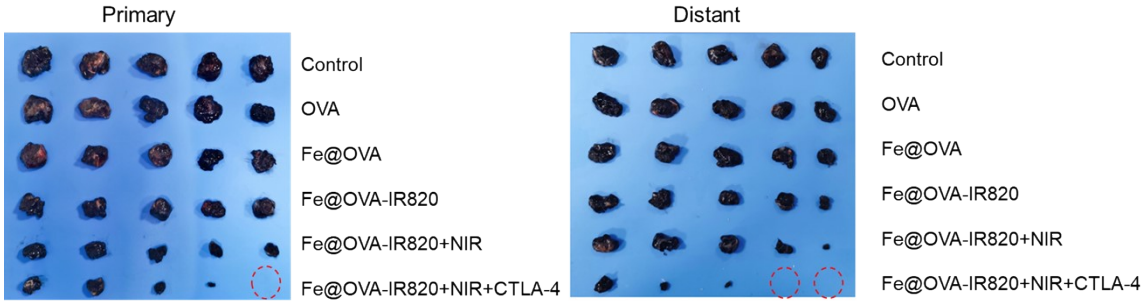

Figure S17. Images of the primary tumor(left) and the distal(right) tumor taken after extraction.

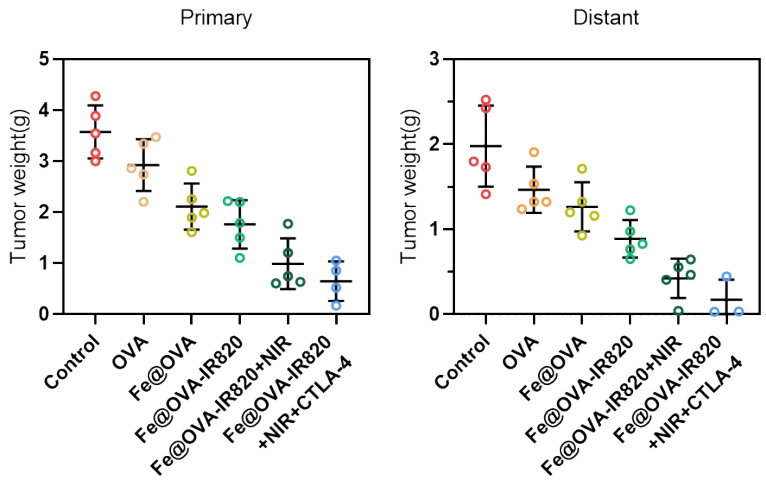

Figure S18. The weight of primary and distant tumors in each group was recorded

after extraction.

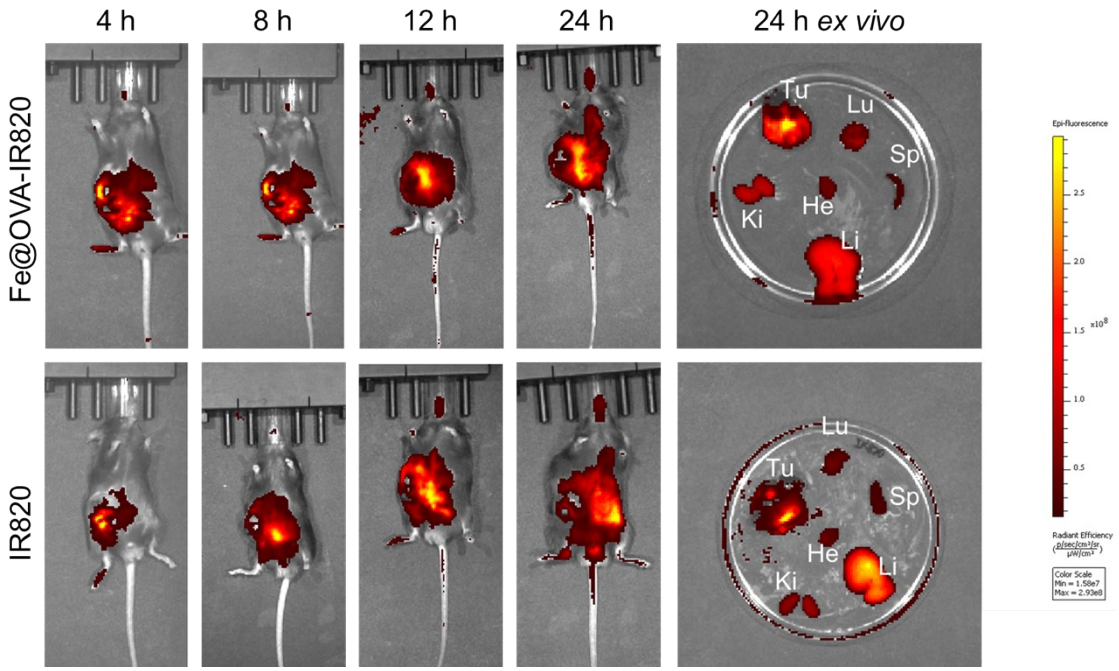

Figure S19. In vivo fluorescence images of mice after Intratumoral injection IR820 and Fe@OVA-IR820 at different time points.

Figure S20. Images of tumor-bearing mice during the treatment process.

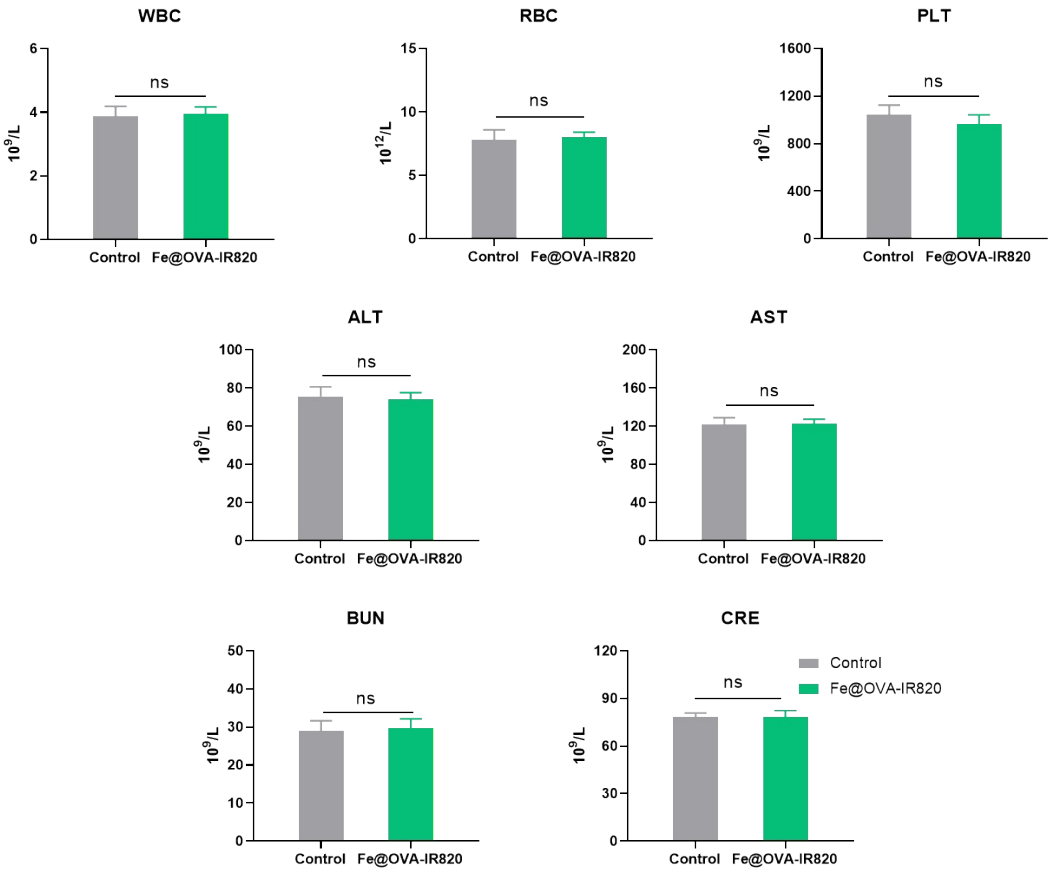

Figure S21. Blood routine examination and serum biochemistry data of mice intravenously administrated with saline, Fe@OVA-IR820. n = 3, Means ± SD. Significance is defined as ns, no significance, *P < 0.05, **P < 0.01, ***P < 0.001.

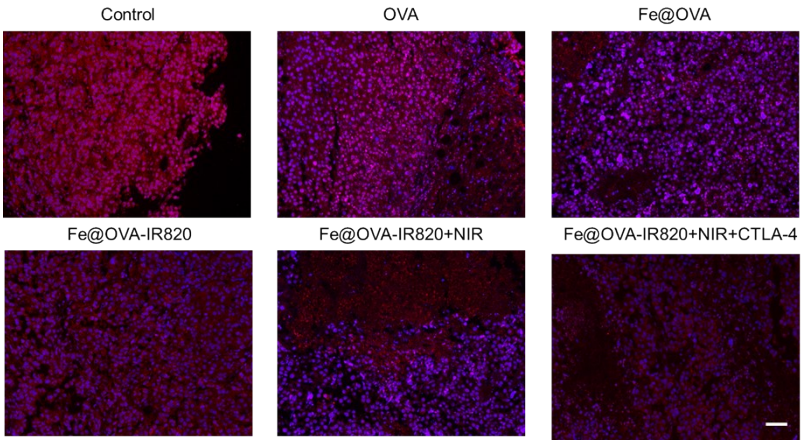

Figure S22. Immunofluorescence staining of GPX4 in tumor sites after various treatments. Scale bar: 100 μm.

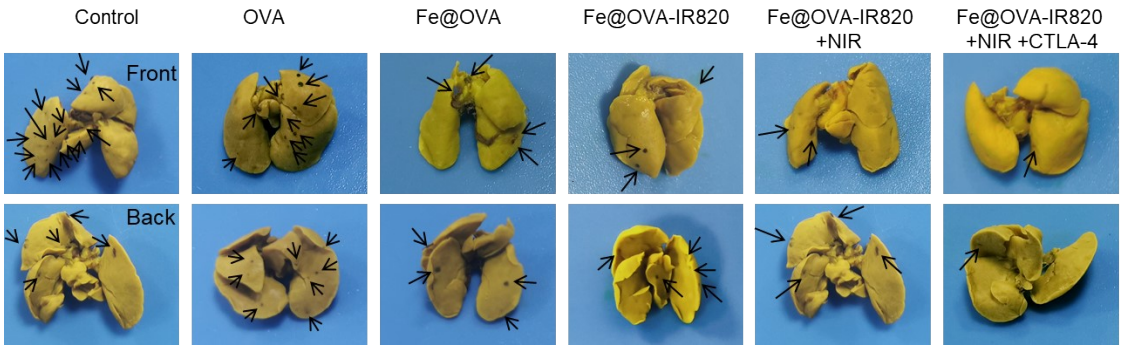

Figure S23. Representative photographs of lung metastasis in B16-OVA tumor model.

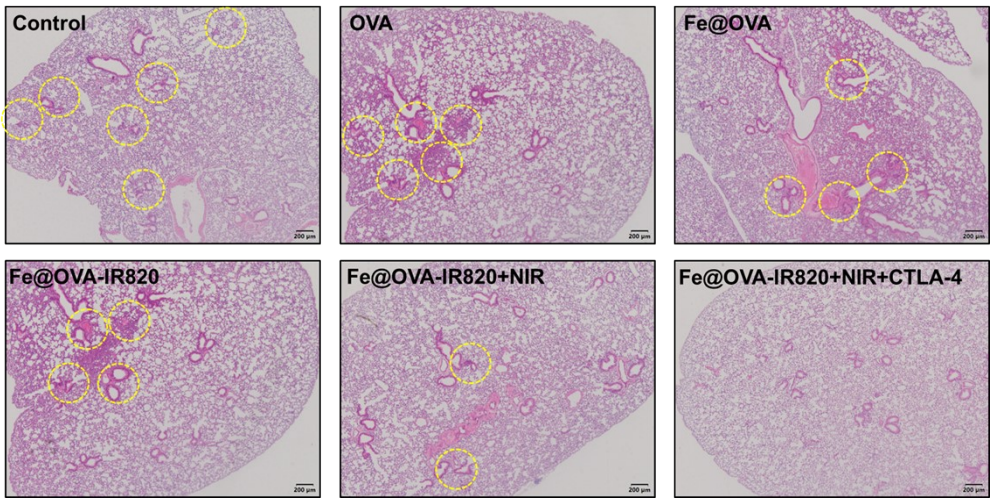

Figure S24. Images of lung tissue collected after light ablation, sections, and hematoxylin-eosin staining. Sites of tumor metastasis are indicated by yellow circles. Scale bar, 200 μm.

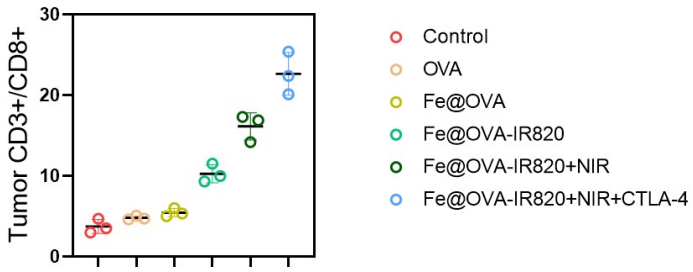

Figure S25. The relative quantification results of T cells (CD3+/CD8+) in Fig. 5C.

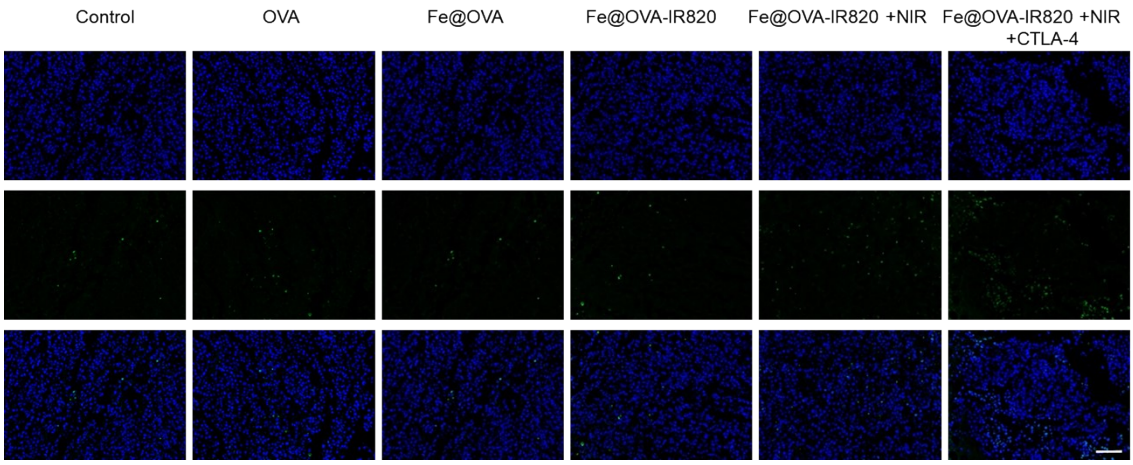

Figure S26. TUNEL staining of tumor tissue images of different groups of tumor sections. Scale: 100 μm.

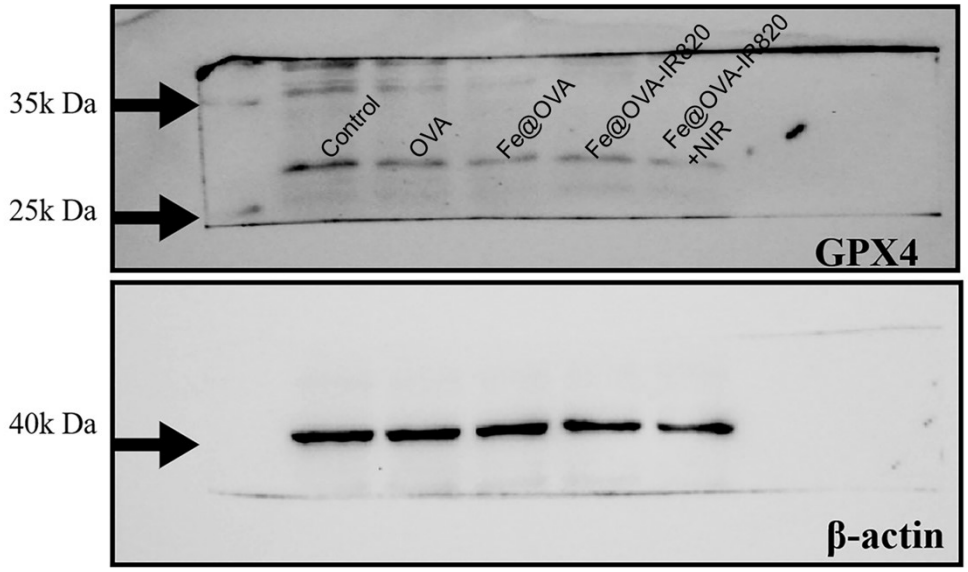

Figure S27. Uncropped images for Figure 2D.